

## PRESENT AND PERSPECTIVES OF THE SPARC THz SOURCE

E. Chiadroni\*, M. Bellaveglia, M. Castellano, G. Di Pirro, A. Drago, M. Ferrario, G. Gatti, E. Pace, C. Vaccarezza, INFN/LNF, Frascati, Italy  
 A. Bacci, A.R. Rossi, INFN/MI, Milano, Italy  
 P. Calvani, O. Limaj, S. Lupi, A. Nucara,  
 Phys. Dept. and INFN University of Rome “La Sapienza”, Italy  
 L. Catani, A. Cianchi, B. Marchetti, INFN “Tor Vergata”, Italy  
 A. Mostacci, L. Palumbo, SBAI Dept. University of Rome “La Sapienza”, Roma, Italy  
 C. Ronsivalle, ENEA C.R. Frascati, Italy

### Abstract

The development of radiation sources in the Terahertz (THz) spectral region has become more and more interesting because of the peculiar characteristics of this radiation: it is non ionizing, it penetrates dielectrics, it is highly absorbed by polar liquids, highly reflected by metals and reveals specific “fingerprint” absorption spectra arising from fundamental physical processes. The THz source at SPARC is a linac-based source for both longitudinal beam diagnostics and research investigations. Its measured peak power is of the order of  $10^8$  W, very competitive with respect to other present sources. The status of the THz radiation source, in particular its generation and properties, is presented and future perspectives are discussed.

### INTRODUCTION

A linac-driven THz radiation is routinely produced at SPARC as Coherent Transition Radiation (CTR) emitted by both an ultra-short high-brightness electron beam and a longitudinally modulated one [1]. The technique used at SPARC to manipulate such electron beam relies on low energy RF compression (the velocity bunching) [2] and on the use of properly shaped trains of UV laser pulses hitting the photo-cathode (comb laser beam) [3], [4].

Recent results on the frequency domain measurements of the THz radiation are presented as longitudinal diagnostics for advanced beam manipulation experiments at SPARC [5]. Several beam configurations have been produced and measured. Here three cases, relevant for THz emission, will be thus discussed, i.e. single bunch (700 fs rms), 2 bunches at 0.8468(0.0008) ps and 4 bunches at 1.65 (0.07) ps separation in a 200 pC train. Since the longitudinal form factor of a distribution of  $n$  bunches equally spaced in the train, is a single line at the comb repetition rate, a very well modulated and periodic comb structure has to be kept down to the TR target to let narrow band coherent THz emission occur.

Novel schemes for the optimization of the narrow band THz source at SPARC are under studying and details can be found in [6].

\* Enrica.Chiadroni@Inf.infn.it

### THEORETICAL BACKGROUND

THz radiation is electromagnetic radiation whose frequency lies between the microwave and infrared regions of the spectrum. In linear accelerators it is generated as coherent radiation emitted from an electron bunch. Each electron in the bunch emits radiation, whose spectrum depends on the Fourier transform of the bunch longitudinal profile, the form factor  $F(\omega)$  [7],  $\omega$  being the emitted frequency. In case of short bunches, the total radiation intensity  $I(\omega) = I_{sp}(\omega)[N + N(N - 1)F(\omega)]$  is dominated by coherent emission and proportional to  $N^2$ , at wavelengths of the order, or longer than the bunch length. Under this condition the longitudinal form factor is  $0 < F(\lambda) \leq 1$ .  $I_{sp}(\omega)$  is the single particle radiation intensity, which depends on the specific emission mechanism. Any kind of source which does not change the electron distribution can be used, e.g. transition radiation (TR), edge radiation from a dipole, undulator radiation, etc. In particular TR, generated when a bunch of relativistic electrons travels through a vacuum-metal interface, is considered here.

The form factor of any kind of electron distribution can be retrieved by means of Fourier transform spectroscopy, based on the fact that the interference pattern (i.e. the interferogram) from a two beams interferometer is the Fourier transform of the radiation passing through it. In particular, for millimeter and sub-millimeter radiation a Martin-Puplett interferometer [8] is usually considered. The beam splitter is a polarizing grid, whose wires are at  $45^\circ$  with respect to the horizontal plane when viewed along the beam axis. The grid reflects the field with polarization parallel to the wires and transmits the orthogonal one. The roof mirrors rotate the polarization of the incident field upon reflection so that the radiation first transmitted by the grid is reflected when it returns, and *vice versa*. The reflected and transmitted components recombine then to produce a total field, at the analyzer grid which splits polarization again into two components, parallel and orthogonal to the wires, whose intensity is detected by the THz detectors. The horizontal and vertical components are  $90^\circ$  out of phase and the amplitudes depend on the phase difference,  $\omega\tau$ , resulting in an elliptically polarized radiation. Assuming a source with an arbitrary intensity distribution,  $I(\omega)$ , the intensity of the

recombined radiation at the detectors can be written as

$$V_{h,v} = \int_0^\infty I(\omega) \left\{ \begin{array}{l} \cos^2\left(\frac{2\omega\tau}{2}\right) \\ \sin^2\left(\frac{2\omega\tau}{2}\right) \end{array} \right\} d\omega. \quad (1)$$

The normalized difference interferogram then can be written as  $\delta(\tau) = \frac{V_h(\tau) - V_v(\tau)}{V_h(\tau) + V_v(\tau)}$  which corresponds to the Fourier transform of the radiation spectrum and it is the measured quantity. The frequency spectrum of the incident radiation pulse can then be obtained by inverse Fourier transforming  $\delta(\tau)$ . The longitudinal form factor is then evaluated from the total radiation intensity.

Fluctuations and drifts in the radiation intensity affect both detector signals in a similar way, whereas the interferograms for the horizontal and the vertical polarization are anticorrelated. At zero optical path distance, the two pulses completely overlap at the detectors and the total intensity reaches the maximum or the minimum, depending on the polarization. As the path difference increases, but is still shorter than the bunch length, the two pulses overlap partially, and the total intensity decreases on one detector while increases on the other. When the path difference of the two arms is larger than the bunch length, the two pulses are totally separated in time and the resulting intensity on each detector is equal. Therefore the baseline of the difference interferogram  $\delta(\tau)$  approaches 0.

For a longitudinally modulated beam the interferogram shows  $2n - 1$  peaks, with  $n$  the number of bunches in the train. Let us consider a 4 sub-pulses radiation pulse, generated by a 4 sub-bunches electron beam. At zero optical path distance each sub-pulse within the two comb trains completely overlap, resulting in the maximum in the difference interferogram. As the path difference increases, the interferogram intensity decreases until three of the four pulses overlap, corresponding to the first side maxima. Increasing the distance, the interferogram intensity decreases again until only two of the sub-pulses super-impose, giving the second side maxima, smaller than the previous ones. Finally, as the distance further increases, only one of the sub-pulses overlaps, giving rise to the last side maxima. The peak separation thus corresponds to the bunches inter-distance in the train. The Fourier transform of the auto-correlation function directly provides information on the resonant frequency of the emission and its bandwidth.

## EXPERIMENTAL APPARATUS

The THz station is placed at the end of the dogleg line, where frequency domain measurements are performed by means of either a Martin-Puplett interferometer or band-pass mesh filters [9], as depicted in Fig.1. A silicon aluminated screen is placed in the vacuum pipe at  $45^\circ$  with respect to the beam axis. The backward CTR radiation, reflected normally to the beam direction, is extracted through a z-cut quartz window. A 152 mm focal length  $90^\circ$  off-axis parabolic mirror, whose focal plane corresponds to the source plane, parallelizes and reflects vertically the radiation beam down towards an aluminum flat mirror, placed at

$45^\circ$  with respect to the horizontal plane. Radiation is then reflected horizontally into the interferometer (the first flat mirror in Fig.1 is moved out in this setup) or to a flat mirror and a second  $90^\circ$  off-axis parabolic mirror in order to be focused onto a Golay cell detector (in this setup the first flat mirror in Fig.1 is moved in).

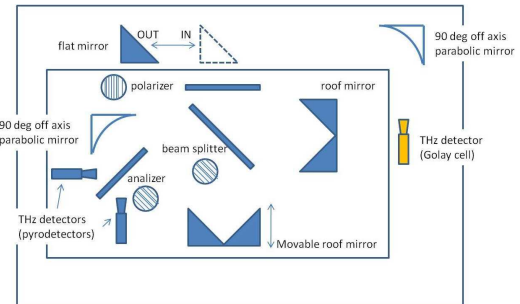


Figure 1: Experimental layout for detection of THz radiation (top view).

In case of autocorrelation measurements, the radiation enters the first polarizer, whose wires are vertical to select horizontal polarization. The horizontally polarized transmitted radiation first reaches the beam splitter (BS), placed at  $45^\circ$ , whose wires are at  $45^\circ$  to the horizontal plane when viewed along the beam input axis. The BS splits the input signal into two equal, orthogonally polarized components, one being reflected towards the stationary roof mirror and the other being transmitted to the moveable one, whose maximum travel distance is 36.7 mm with a minimum step width less than  $1 \mu\text{m}$ . Radiation coming back from both arms to the beam splitter recombines, being then focused by a  $90^\circ$  off-axis parabolic mirror onto the pyroelectric detectors via the analyzing wiregrid, located between the mirror and the pyroelectric detectors. Wire grids are wound from  $10 \mu\text{m}$  diameter thick tungsten wire with a spacing of  $20 \mu\text{m}$ .

The total emitted radiation amplitude for narrow band measurements can be detected by means of a band-pass filter with characteristic frequency of 1.5 THz, placed in front of Golay cell detector.

## RESULTS

The SPARC THz source has been characterized in different schemes, i.e. single bunch and laser comb (2 and 4 bunches in the train), in order to exploit different regimes of coherent THz emission, i.e. broad band and narrow band, respectively.

While the production and transport, down to the linac exit, of a train of bunches with THz repetition rate has been successfully achieved, even if challenging due to the high charge stored in each bunch, the transport through the dogleg down to the THz station of such a longitudinally modulated beam is dramatically affected by several parameters, e.g. beam energy spread,  $R_{56}$  of the beamline, etc., re-

sulting in a degradation of the comb structure, and consequently in a widening of the THz emission bandwidth.

In all the cases presented here, the beam energy was around 110 MeV and beam charge 200 pC.

The frequency dependence of TR single particle spectrum, the detectors response and the transmission of both filter and z-cut quartz window have been taken into account to estimate the radiation energy in the range of THz emission, i.e. 0.15 - 2 THz, for the beam configuration used.

Since the full width at half maximum (FWHM) of the autocorrelation function is proportional to the FWHM of the pulse, a rough analysis of the single bunch can be done by assuming the pulse shape is known. Fitting the normalized difference interferogram, it is possible to find the rms bunch length and the cut-off frequency of the interferometer [10]. As pointed out from the fit (Fig.2), the RMS bunch

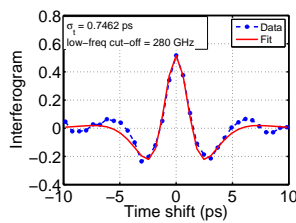


Figure 2: Difference interferogram (blue dots) and analytical fitting function (red curve) to account for the high-pass filter behavior of the interferometer.

length measured at the THz station is greater than the one measured at the end of the linac by a factor 3, due to the lengthening induced by the transport through the dogleg.

In the two bunches operation, in order to select the CTR emission at the THz frequency and enhance its intensity, the pulse distance has been optimized and the profile shrunk by RF compression. The measured form factor is shown in Fig.3a), exhibiting a well defined peak around the resonant frequency of the comb distribution, i.e. 1.2 THz.

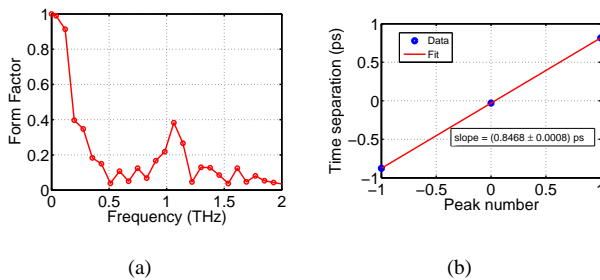


Figure 3: Form factor (a) and bunch separation (b) for the two bunches beam.

For a four bunches comb distribution, the proper pulse spacing and length for suitable narrow band THz generation has been found in the so-called deeply over-compression regime, in which all the sub-bunches are debunching at the exit of the linac, thus well separated in time

(Fig.4a). For such a longitudinal distribution, the interferogram is multi-peaked (Fig.4b), whose time distance corresponds to the separation of the bunches in the train (Fig.4c). The retrieved form factor (Fig.4d) is then peaked at the comb repetition frequency, whose bandwidth depends on both the modulation of the bunches in the train and their length.

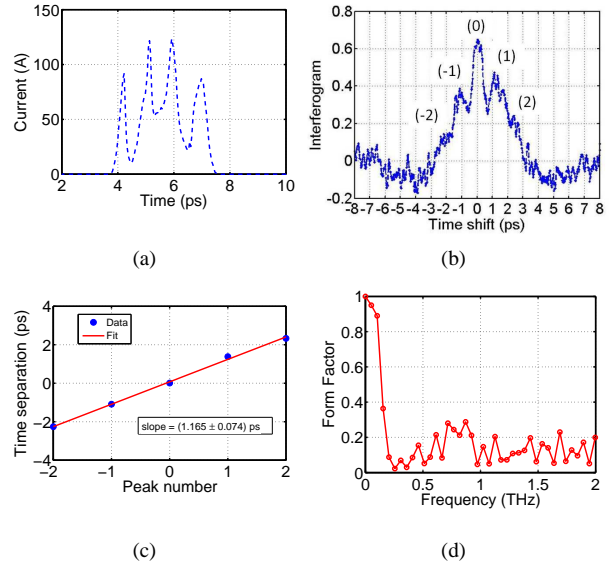


Figure 4: Multi-peaked interferogram (b), form factor (c) and bunch separation in the train (d) for a 4 bunches comb beam (a).

## CONCLUSIONS

A linac-driven high intensity THz radiation is produced at SPARC taking advantage of the high brightness electron beams. Two main schemes are currently investigated, ultra-short single bunch and multi-bunches comb beams, to generate high power broadband or narrowband THz radiation, respectively. Further analysis is ongoing in order to evaluate the properties of the THz radiation so generated.

## REFERENCES

- [1] E. Chiodroni *et al.*, Proc. of IPAC10, TUOARA03 (2010).
- [2] M. Ferrario *et al.*, Phys. Rev. Lett. **104**, 054801 (2010).
- [3] P. O'Shea *et al.*, Proc. of PAC01, p.704 (2001).
- [4] M. Boscolo *et al.*, NIM A **577**, 409-416 (2007).
- [5] A. Mostacci *et al.*, Proc. of IPAC11, THYB01 (2011).
- [6] B. Marchetti *et al.*, Proc. of IPAC11, THPS104 (2011).
- [7] R. Lai, A.J. Sievers, NIM A **397**, 221-231 (1997).
- [8] D. H. Martin and E. Puppelt, Infrared Physics, vol. 10, pp. 105-109 (1970).
- [9] N. I. Landy, 1-4244-1449-0/07/\$25.00 c 2007 IEEE (2007); P. Carelli *et al.*, unpublished (arXiv:0907.3620v2).
- [10] J. Rosenzweig *et al.*, CTR-based diagnosis of electron beam pulse shape, 8<sup>th</sup> Advanced Accelerator Concepts Workshop (1999).